Trans. of the Society of Instrument and Control Engineers
Vol.E-2, No.1, 33/41 (2002)

High Accuracy Control of Industrial Articulated Robot Arms with Trajectory Allowance Under Torque and Speed Constraint: Trajectory Generation and Taught Data Generation

Masatoshi NAKAMURA*, Takuya IWANAGA*,
Satoru GOTO* and Nobuhiro KYURA**

High speed and high accurate control performance is required for industrial robot arms. The research is aimed at high accurate control of industrial articulated robot arms with trajectory allowance under torque and speed constraints. The proposed method is based on nonlinear separation that decomposes the nonlinear dynamics from the nonlinear static parts and linear dynamic part. Controller was constructed for separation of trajectory generation and taught data generation, and it could be achieved perfect performance under the speed and torque constraints imposed by the hardware of robot arm. The effectiveness of the proposed method was assured by experimental results of an actual articulated robot arm.

Key Words: Industrial articulated robot arms, Trajectory allowance, Torque constraint, Speed constraint, High accurate control

1. Introduction

Industrial robot arms are used in various works such as assembling, transporting, handling, welding, burring, grinding. High speed and high accurate control of industrial robot arms are required to increase efficiency and precision. Current constraint of power amplifiers, torque constraint of motors and characteristic difference of each link are the problems of control of industrial robot arms. The problems cause deterioration of control performance such as the presence of overshoot in following locus.

Actuator saturation problems were investigated in 1)∼3), however, most of them are feedback type controller and it is not easy for applying them to industrial robot arms because hardware changes are required [4), 5)]. On the other hand, we have proposed control methods of industrial robot arms such as accurate contour control without change of hardware by using Gaussian network [6)], upper limit of contour control performance with torque constraint [7)], minimum time positioning control considering locus error and torque constraints [8)] and contour control method under speed and torque constraints [9)].

The minimum time positioning control method considering locus error under torque constraints gives input trajectory of the shortest distance from starting point to end point with maximum speed under torque constraint. The contour control method under speed and torque constraints approximates corner part in objective locus by circular arc and it gives input trajectory with assigned velocity under torque constraint. However, in actual works, some allowance of the end-effector motion exists in order to avoid obstacles and contact with workpieces, then work space has many special constraints even in positioning control case.

In this paper, high accurate control of industrial robot arms with trajectory allowance under torque and speed constraint is proposed. In the proposed method, objective trajectory generation and taught data generation are completely separated based on the nonlinear separation control concept which separates the nonlinear dynamic controlled object into nonlinear static part and linear dynamic part [10)]. The proposed method appropriately satisfies the constraints of torque and speed in the robot arm hardware.

Feedback type controller usually requires a change of hardware in the robot arms. As the proposed method is a feedforward type controller, it requires no change of the hardware and hence it is easy to apply it to industrial fields.

2. Control System of Articulated Robot Arm

2.1 Structure of articulated robot arm

Fig. 1 shows the two-degree-of-freedom articulated

* Graduate School of Science and Engineering, Saga University, Saga
** Faculty of Engineering in Kyushu, Kinki University, Iizuka

robot arm which moves in the X-Y plane using the first link and the second link. In Fig. 1, (θ_1, θ_2) shows the joint angles in the joint coordinate space whereas (x, y) shows the end-effector position in the working coordinates. L_1 and L_2 show the lengths of the first link and that of the second link, respectively, and the symbol ○ shows the joints.

2.2 Problems in control design

Torque constraint of the motors in the joint coordinates and speed constraint of the end-effector in the working coordinates are restrictions for control design of articulated robot arms. If the constraints could not be satisfied, control performance of the robot arm deteriorates seriously and work specifications are not acceptable. Hence, the robot arm must move under these constraints.

The torque constraint in the joint coordinates can be expressed by the joint acceleration constraint considering about the motor axis as the maximum equivalent moment of inertia

$$|a_j| < a_{max} \tag{1}$$

where a_j $(j = 1, 2)$ and a_{max} are the angular acceleration of joint j and the maximum joint acceleration, respectively. The speed constraint of the end-effector in the working coordinates is given by

$$|v_e| < v_{max} \tag{2}$$

where v_e and v_{max} are the end-effector velocity and the speed constraint, respectively.

In this way, the torque constraint (1) and the speed constraint (2) must be take into account for the control design of the articulated robot arms.

In industrial applications, the end-effector motion within some allowable region is enough to achieve acceptable performance in industrial robot arms. The maximum width of the allowance is given by

$$|w| \le w_{max} \tag{3}$$

where w and w_{max} are allowance and its maximum width, respectively.

In this research, the controller is designed such that the constraints (1), (2) and (3) are fulfilled.

2.3 Model of articulated robot arm based on nonlinear separation control

In this research, nonlinear separation model for articulated robot arm is constructed [10]. In this model, robot arm mechanism is considered as a nonlinear static part and robot arm dynamics is as a linear dynamic part. In the nonlinear static part, objective trajectory under torque and speed constraints is generated, and in the linear dynamic part, taught data are generated based on the second order model of the robot arm dynamics in the joint coordinates.

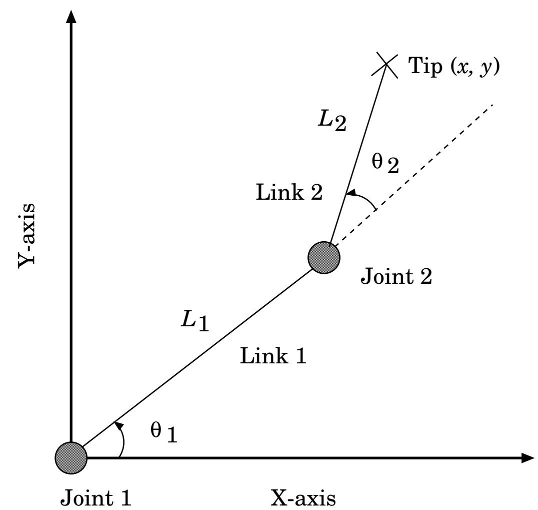

Fig. 1 Structure of two-degree-of-freedom robot arm

In the nonlinear static part, the robot arm mechanism is expressed by the kinematics transformation from (θ_1, θ_2) in the joint coordinates to (x, y) in the working coordinates as

$$x = L_1 \cos\theta_1 + L_2 \cos(\theta_1 + \theta_2) \tag{4}$$

$$y = L_1 \sin\theta_1 + L_2 \sin(\theta_1 + \theta_2) \tag{5}$$

and the inverse kinematics transfors from (x, y) to (θ_1, θ_2) as

$$\theta_1 = \sin^{-1}\left(\frac{y}{\sqrt{x^2+y^2}}\right) - \sin^{-1}\left(\frac{L_2 \sin\theta_2}{\sqrt{x^2+y^2}}\right) \tag{6}$$

$$\theta_2 = \pm\cos^{-1}\left(\frac{x^2+y^2-(L_1)^2-(L_2)^2}{2L_1L_2}\right) \tag{7}$$

(See Fig. 1).

Almost all industrial robot arms are controlled in the joint coordinates [12]. Kinematic control of industrial robot arms is based on the de-coupled, linear joint model, which is widely used in today's robotic industry.

Industrial robot arms are employed in pre-determined operations. The non-linear torque disturbances such as centripetal and Coriolis as well as gravity loading can be quantifiable. These non-linearities are usually controlled by appropriate mechanical design such as parallel linkage and PI type controllers.

Under normal speed condition which is below about 1/5 of the rated motor speed, joint dynamics could be descried by the second order linear model, which is given by

$$\frac{d^2\theta(t)}{dt^2} = sat\left(K_v\left(K_p\big(u(t)-\theta(t)\big) - \frac{d\theta(t)}{dt}\right)\right) \tag{8}$$

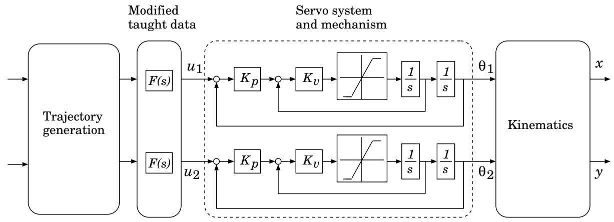

Fig. 2 Block diagram of the proposed method

where $sat(z)$ shows the torque constraint as

$$sat(z) = \begin{cases} a_{max} & (a_{max} < z) \\ z & (-a_{max} \leq z \leq a_{max}) \\ -a_{max} & (z < -a_{max}) \end{cases} \tag{9}$$

In (8), K_p is the position loop gain, K_v the velocity loop gain, $u(t)$ angle input and $\theta(t)$ angle output. In (9), a_{max} is maximum joint acceleration as in (1). The torque constraint is calculated by the multiplication of a_{max} and the motor axis equivalent moment of inertia.

Under the torque constraint, $sat(\cdot)$ in (8) can be neglected and the robot arm dynamics is expressed by

$$\theta(s) = \frac{K_v K_p}{s^2 + K_v s + K_v K_p} U(s) \tag{10}$$

in s domain. Eq. (10) shows the linear dynamics of the articulated robot arm in the joint coordinates.

3. Control Method of Articulated Robot Arm Based on Nonlinear Separation

3.1 Objective trajectory generation within allowance

Objective trajectory of robot arm is generated under speed and torque constraints. Trajectory generation is treated as the compensation in the nonlinear static part because it focuses on the static characteristics of the robot arm.

One of the requirements of positioning control for articulated robot arms is shortening operation time. For avoiding obstacles in handling works or spot welding motion between dotting interval, allowance is introduced to the end-effector motion and the objective locus is determined such that minimum operational time under the allowance can be realized. The objective trajectory of the minimum time motion is generated from the objective locus under speed and torque constraints.

The objective trajectory generation within the allowance is obtained by the following procedure.

(1) Starting point A_0, intermediate point A_1, end point A_2 are assigned as shown in **Fig. 3** and the allowance is set from the assigned points A_0, A_1, A_2. The screening part in Fig. 3 shows the allowance of width w.

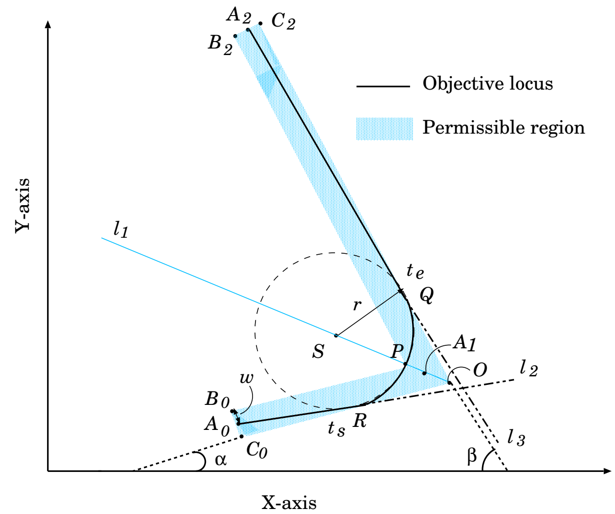

Fig. 3 Trajectory generation with allowance

(2) To reduce the torque requirement and to increase speed, the objective locus is generated such that the locus draws a curve within the allowance at the corner part. The generation procedure is explained as follows;

(I) The circle which goes through the point P and is tangent to the straight line C_0O, C_2O, is obtained as

$$(x - x_c)^2 + (y - y_c)^2 = r^2 \tag{11}$$

where (x_c, y_c) and r are the center point and the radius of the circle, respectively.

(II) The straight line l_2 which draws through the starting point A_0 and is tangent to the circle (11), and the straight line l_3 which draws through the end point A_2 and tangent to the circle (11), are obtained as

$$l_2\colon y = m_6 x + n_6 \tag{12}$$

$$l_3\colon y = m_7 x + n_7 \tag{13}$$

where m_6 and n_6 are the gradient and the intercept of the straight line l_2, respectively, and m_7 and n_7 are for the straight line l_3.

By connecting (11), (12) and (13), the objective locus is generated (see Appendix A).

(3) The objective trajectory is generated from the objective locus by considering the torque and speed constraints. (see **Fig. 4**).

(I) The corner is approximated by circlar arc. The radius of the circle determines the moving speed. The objective trajectory at the corner part is derived by

$$x(t) = x(t_s) + r[\sin(\alpha + v_g(t - t_s)/r) - \sin\alpha]$$

$$(t_s \leq t < t_e) \quad (14)$$

$$y(t) = y(t_s) + r[\cos\alpha - \cos(\alpha + v_g(t - t_s)/r)]$$

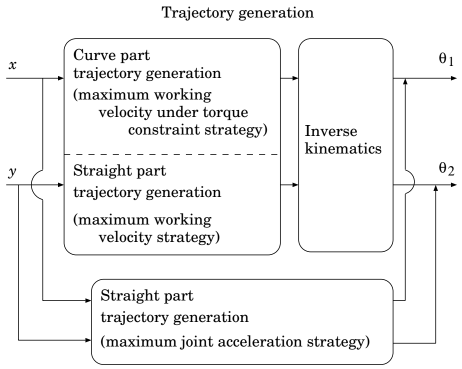

Fig. 4 Block diagram of trajectory generation

$$(t_s \le t < t_e) \qquad (15)$$

$$v_g = \sqrt{A_{max} r}$$

where α is the angle between the straight line C_0O and X-axis, and t_s, t_e are the time at the tangential point of the circle and the line l_2 and that at the tangential point of the circle and the line l_3, respectively. A_{max} is the maximum acceleration under the torque constant and it is determined by simulation study. Generated objective trajectory given by (14), (15) in the working coordinates is transformed into that in the joint coordinates through the inverse kinematics (6) and (7).

(II) The objective trajectory at straight line part is generated by the following procedure. The objective trajectory at straight line part is divided into the segnemts of the maximum joint acceleration and that of the maximum speed in the working coordinates within the speed constraint. The minimum time motion control can be achieved with the maximum joint acceleration until the maximum speed is reached.

i. At the maximum joint acceleration part, the straight line is segmented by a set of equidistant knot points k ($k = 0, 1, 2, \cdots n-1$) and the objective trajectory moves between the knot point k and $k+1$ at the maximum joint acceleration as

$$\theta_j(t_k + t) = \theta_{j,k} + \dot{\theta}_{j,k} t + \ddot{\theta}_{j,k} t^2/2 \qquad (0 \le t \le t_{k+1} - t_k) \qquad (16)$$

where $\theta_{j,k}$, $\dot{\theta}_{j,k}$ and $\ddot{\theta}_{j,k}$ are the joint angle, the first order derivative and the second order derivative for the jth axis at kth step, and t_k is the time at the knot point k.

ii. For determining the switching time form the maximum joint acceleration part to the maximum speed part, the tangential velocity in the working coordinates must be calculated for the maximum joint acceleration part. The relationship between the joint velocity and the end-effector velocity is

$$\begin{pmatrix} \dot{x} \\ \dot{y} \end{pmatrix} = J \begin{pmatrix} \dot{\theta}_1 \\ \dot{\theta}_2 \end{pmatrix}$$

$$v_e = \sqrt{\dot{x}^2 + \dot{y}^2}$$

where v_e is the tangential velocity at θ_1, θ_2 and Jacobian J is given by

$$J = \begin{bmatrix} L_1 \cos\theta_1 + L_1 \cos(\theta_1 + \theta_2) & L_2 \cos(\theta_1 + \theta_2) \\ -L_1 \sin\theta_1 - L_2 \sin(\theta_1 + \theta_2) & -L_2 \sin(\theta_1 + \theta_2) \end{bmatrix}$$

iii. At the maximum speed in the working coordinates within the speed constraint, the working trajectory is derived by

$$x(t) = x(t_\rho) + \dot{x}(t_\rho)(t - t_\rho) + A_c \cos\phi (t - t_\rho)^2/2 \quad (t_\rho \le t \le t_\sigma) \; (17)$$

$$y(t) = y(t_\rho) + \dot{y}(t_\rho)(t - t_\rho) + A_c \sin\phi (t - t_\rho)^2/2 \quad (t_\rho \le t \le t_\sigma) \; (18)$$

where A_c is the end-effector acceleration in the working coordinates, t_ρ and t_σ are the time just before the speed constraint and the time just after the speed constraint, respectively and $\phi = \sin^{-1}((y(t_\sigma) - y(t_\rho))/l_c)$.

The objective trajectory (17), (18) in the working coordinates is transformed into the joint trajectory by the inverse kinematics (6), (7).

Hereby, the objective trajectory at the straight line part is generated (see Appendix B).

According to the above procedure, the objective trajectory within the torque and the speed constraints is generated, which corresponds to the nonlinear static compensation part.

3.2 Modified taught data from objective trajectory

To compensate the delay of dynamics, the objective trajectory is modified by the modified taught data method based on the second order model of the mechatronic servo system [11] as shown in **Fig. 2** of surrounded part by dotted line. The compensation corresponds to the control of linear dynamics in the nonlinear separation control.

Delay compensated trajectory is used as the input of the servo controller in real-time operation. The modification term $F(s)$ for each axis in Fig. 2 is designed by the pole assignment regulator and the minimum order observer as

$$F(s) = \frac{q_3 s^3 + q_2 s^2 + q_1 s + q_0}{(s - \mu_1)(s - \mu_2)(s - \gamma)} \qquad (19)$$

in that numerator coefficients are

$$q_0 = -\mu_1 \mu_2 \gamma$$

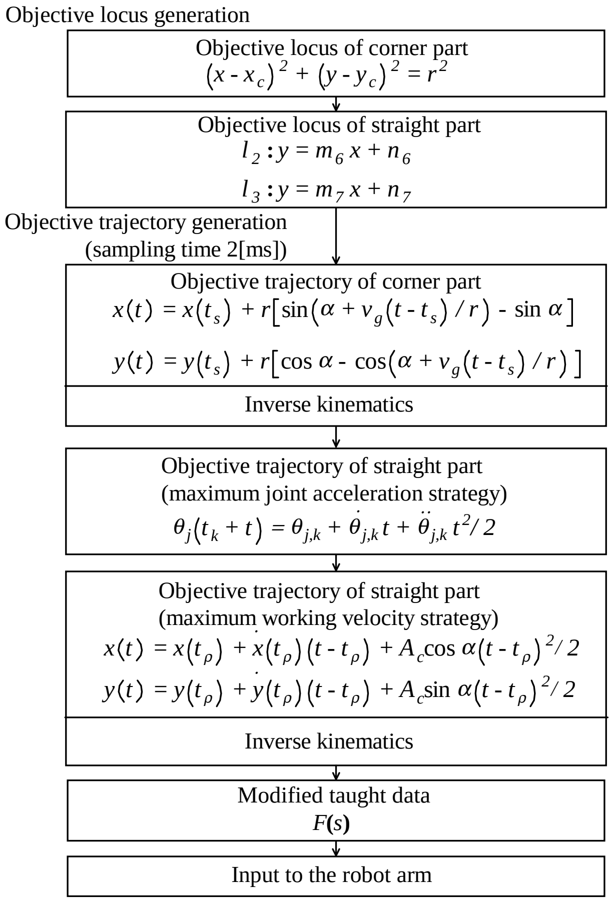

Fig. 5 Flowchart of the proposed high speed control algorithm

$$
\begin{aligned}
q_1 &= (K_v + \gamma)(\mu_1 + \mu_2) + (K_v)^2 + \mu_1\mu_2 \\
&\quad + K_v\gamma - \frac{\mu_1\mu_2\gamma}{K_p} \\
q_2 &= \frac{1}{K_p}(K_v + \gamma)(\mu_1 + \mu_2) + (K_v)^2 + \mu_1\mu_2 \\
&\quad + K_v\gamma - \frac{\mu_1\mu_2\gamma}{K_p K_v} \\
q_3 &= \frac{1}{K_p K_v}(K_v + \gamma)(\mu_1 + \mu_2) + (K_v)^2 + \mu_1\mu_2 + K_v\gamma
\end{aligned}
$$

where μ_1, μ_2 regulator poles, and γ is the observer pole.

3.3 Algorithm of control method based on nonlinear separation control

Flowchart of the proposed control method with allowance is shown in **Fig. 5**.

1. The objective locus (11), (12) and (13) is generated for the purpose of reduction of torque at the corner part.
2. The objective trajectory (14), (15), (16), (17) and (18) is generated from the objective locus. (Sampling time interval is 2[ms].)
3. The objective trajectory is transformed from the working coordinates to the joint coordinates by the inverse kinematics (6) and (7).

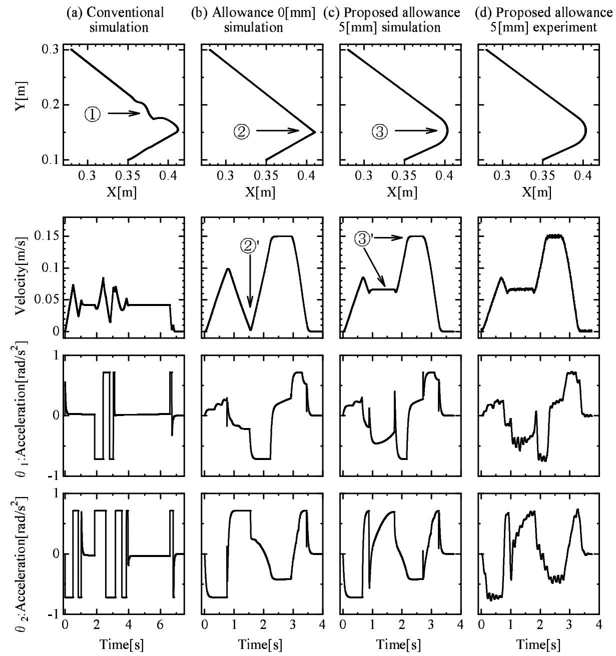

Fig. 6 Simulation and experimental results (a) simulation result of the conventional method (b) simulation result of allowance 0[mm] (c) simulation result of the proposed method allowance 5[mm] (d) experimental result of the proposed method allowance 5[mm]

4. Delay of the joint dynamics is compensated by the modification term (19).
5. The taught data is input to the robot arm at each reference input time interval 2[ms].

4. Verification of Control Method of Articulated Robot Arm Based on Nonlinear Separation Control

4.1 Experimental conditions

The proposed control method is applied to an articulated robot arm PERFORMER-MK3S (Yahata Electric Mfg. Co. Ltd.). Articlated robot arm PERFORMER-MK3S has a 5 degree-of-freedom. L axis and U axis are used for experiments. Servo motor of each joint connects to the servo controller which controls current and velocity of the servo motor. The servo controller connects to the computer which controls position angle of the servo motor. AC servo motor of the rated speed 3000[rpm] is used as the actuator of the robot arm where it connects to the arm through reduction gears.

Specifications of the robot arm could be stated as follows: position loop gain $K_p = 25$[1/s], velocity loop gain $K_v = 150$[1/s], lengths of the arm $L_1 = 0.25$[m], $L_2 = 0.215$[m], gear ratios of axes $n_1 = 160, n_2 = 161$, the maximum joint acceleration $a_{max} = 0.72$[rad/s^2] corresponding to the torque constraint (1), the maximum torque constraint acceleration $A_{max} = 0.09[\mathrm{m/s^2}]$, the maximum speed $v_{max} = 0.15[\mathrm{m/s}]$ corresponding to the speed constraint (2), sampling time interval $\Delta t = 2[\mathrm{ms}]$, the starting point $A_0 = (0.35, 0.10)$, the intermediate point $A_1 = (0.41, 0.15)$, the end point $A_2 = (0.28, 0.30)$ and the allowance $w = 5[\mathrm{mm}]$ corresponding to (3).

Experiment method is explained as follows. The difference between the objective position input and the servo motor position output, multiplied by the position loop gain K_p is inputted as the velocity input to the servo controller through D/A converter. The servo motor position output is obtained by the numerical integration of the velocity output. The velocity output is calculated in the servo controller by F/V conversion of pulse output of the servo motor. The end-effector position can not be measured because no sensor is attached to the end-effector. Hence, the joint angle output is used to derivate the end-effector position using kinematics, and the calculated end-effector position is used for the evaluation of control performance.

4.2 Experimental results

Fig. 6 shows locus, tangential velocity, angular acceleration for each axis of (a) Simulation of conventional method, (b) Simulation of the proposed method with zero allowance 0[mm], (c) Simulation of the proposed method with an allowance of 5[mm], (d) Experiment of the proposed method with an allowance of 5[mm]. Here, the conventional method has no allowance and no modification of taught data with the maximum speed. At the simulation result of the conventional method, the maximum error between the objective locus and the following locus was 7.18[mm] and the mean error was 2.39[mm] which was affected by the torque saturation as shown in ① of Fig. 6 (a). In the simulation result of the proposed method with allowance of 5[mm], the maximum error was 0.27[mm] and the mean error was 0.12[mm] as shown in ③. During the entire operational time, high speed operation was obtained by using the proposed method. The experimental result of the proposed method is almost same as the simulation result and thereby the effectiveness of the proposed method was verified.

4.3 Relationship between allowance and operating time

Effectiveness for the allowance of the proposed method is assured by the simulation results with the allowance (a) 0[mm] and (c) 5[mm]. At 0[mm] case, the corner part was sharp and the tangential velocity was almost 0[m/s] as shown in ② and ②' of Fig. 6 (b). On the other hand, at 5[mm] case, the corner part was gentle and the tangential velocity was 0.055[m/s] as shown in ③ and ③' of Fig. 6 (c). Total operating times having the allowance 0[mm] and 5[mm] were 3.55[s] and 3.34[s], respectively. The results show that the allowance reduces speed variation and keeps high speed. Vibration of the end-effector and load of robot arms are reduced, and the operating time is also reduced.

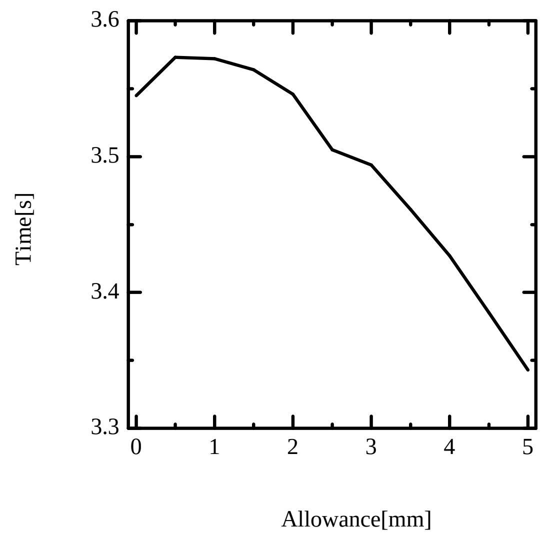

Fig. 7 Relation of allowance and time

Next, the relationship between the allowance and the operating time is shown in **Fig. 7**. The operating time with the allowance 2[mm] is shorter than that of 0[mm]. This is caused by the fact that the velocity at the corner part could not be increased for the small allowance. However, introduction of the allowance gives the effects of vibration and load reduction. Over 2[mm], the operating time can be shorten. The result provides strong evidence for shows the effectiveness of the proposed method.

4.4 Discussion

The proposed method was based on the nonlinear separation control. The control design was done as the objective trajectory generation including torque and speed constraints as a nonlinear static part, and the taught data generation on the basis of second order model of mechatronic servo system as a linear dynamic part.

In comparison with conventional method in Fig. 6 (a) and the proposed method (c), the proposed method gives high moving speed and small deterioration of the following locus. This is because the objective trajectory is generated in consideration of the torque and the speed constraints for the objective locus. From that, the proposed method realizes the specifications of robot arm appropriately.

By comparing experiment in Fig. 6 (d) with simulation (c), these results were coincided. The simulation result is based on theory and it is exactly comparable with experiment. It confirms that the theory can precisely explain the actual results.

5. Conclusion

High accurate control method with trajectory allowance under torque and speed constraints for articulated robot arms was proposed. The proposed method was based on the nonlinear separation control which separated control object into the nonlinear static part and the linear dynamic part. Control design for the nonlinear static part was the objective trajectory generation and the inverse kinematics. The linear dynamic part was the taught data generation and delay dynamics compensation. The proposed method can adequately realize specifications of robot arm and the effectiveness of the method was assured by simulation and experimental results. The proposed method modifies the input of robot arms and it does not need any change in hardware, and it can realize the highest control performance of the robot arms not only for two-degree-of-freedom but also multiple-degrees-of-freedom. Hence, the proposed method is easily and effectively applicable to the industrial field.

References

1) C. W. Chan and K. Hui: Actuator Saturation Compensation for Self-Tuning Controllers, *Int. J. Control*, **59**–2, 543/560 (1994).
2) R. Watanabe, K. Uchida, E. Shimemura and M. Fujita: A New Synthesis of Anti-Windup and Bumpless Transfer for Systems with Constraint on Control Inputs, *Trans. of SICE*, **30**–6, 660/668 (1994).
3) S. Vichai and M. Nakano: A Position Control Using Time Scale with Considering Constraint of Control Signal, *Trans. of SICE*, **30**–7, 742/750 (1994).
4) T. Okita: Real Intension and Official Stance of Motion Control, The Value of Motion Control from a Point of View of a Young Developer, *The Institute of Electrical Engineering of Japan Transactions on Industry Applications*, **120D**–2, 304 (2000).
5) T. Nakatsuka: Real Intension and Official Stance of Motion Control, Actual Reasons on Using PID Controller, *The Institute of Electrical Engineering of Japan Transactions on Industry Applications*, **120D**–3, 467 (2000).
6) S. Goto, M. Nakamura and N. Kyura: Accurate Contour Control of Mechatronic Servo Systems Using Gaussian Networks, *IEEE Transaction Industrial Electronics*, **43**–4, 469/476 (1996).
7) M. Nakamura, S. Aoki, S. Goto and N. Kyura: Upper Limit of Performance for Contour Control of Industrial Articulated Robot Arm with Torque Constraints and Its Realization, *Trans. of SICE*, **35**–1, 122/129 (1999).
8) M. Nakamura, S. Aoki, S. Goto and N. Kyura: Minimum Time Positioning Control of Industrial Articulated Robot Arm Considering Locus Error under Torque Constraints, *Journal of the Japan Society for Precision Engineering*, **66**–3, 451/457 (2000).
9) M. Nakamura, S. R. Munasinghe, S. Goto and N. Kyura: Feasible Method of Optimum Control of Industrial Robot Arms in Operation Under Speed and Torque Constraints, *3rd Asian Control Conference* (2000).
10) M. Nakamura, S. Goto, T. Sugi: A Methodology for Designing Controllers for Industrial Systems Based on Nonlinear Separation Model and Control, *Control Engineering Practice* , **7**–3, 347/356 (1999).
11) M. Nakamura, S. Goto and N. Kyura: Accurate Contour Control of Industrial Articulated Robots by Modified Taught Data Method Based on Nonlinear Separation, *Trans. of SICE*, **36**–1, 68/74 (2000).
12) M. Nakamura, S. Goto and N. Kyura: *Control of Mechatronic Servo Systems*, Morikita Shuppan (1998).
13) J. Zou, M. Nakamura, S. Goto and N. Kyura: Model Construction and Servo Parameter Determination of Industrial Mechatronic Servo Systems Based on Contour Control Performance, *Journal of the Japan Society for Precision Engineering*, **64**–8, 1158/1164 (1998).

Appendix A. Derivation of Objective Locus with Allowance

For the objective locus generation with allowance, high speed operation can be realized by lengthening the radius of circular arc at the corner part

In **Fig.** 3, the starting point $A_0(x_0, y_0)$, the intermediate point $A_1(x_1, y_1)$, the end point $A_2(x_2, y_2)$ and the allowance $w(= A_0B_0 = A_0C_0 = A_2B_2 = A_2C_2)$ are given. Procedure of the objective locus trajectory generation is as follows:

1. The straight lines C_0O, C_2O, B_0P, B_2P which express the allowance, and the point P which is gone through the objective locus are derived.

(i) The straight lines C_0O, C_2O, B_0P and B_2P

Points B_0, C_0, B_2, C_2 are derived form the starting point A_0, the intermediate point A_1, the end point A_2 and allowance w. The equations of straight lines C_0O, C_2O, B_0P, B_2P are derived by

$$C_0O : y = m_1x + n_1 \tag{A. 1}$$

$$C_2O : y = m_2x + n_2 \tag{A. 2}$$

$$B_0P : y = m_3x + n_3 \tag{A. 3}$$

$$B_2P : y = m_4x + n_4 \tag{A. 4}$$

(ii) The point P is obtained from (A. 3) and (A. 4) as

$$P = (x_3, y_3)$$

2. The objective locus of the straight lines l_2, l_3 and the circular arc with center point S are determined.

(i) The bisected straight line l_1 with the allowance is derived by

$$l_1 : y = m_5x + n_5 \tag{A. 5}$$

(ii) The circle which contacts with the straight line C_0O and C_2O, and goes through the point P is derived.

The center point S of the circle lies on the straight line l_1 and its coordinates could be expressed as $S(x, m_5x + n_5)$. The circle goes through the point of tangenct Q with the straight line C_2O and the point of intersection between the arc and line l_1, then $SP = SQ$. The circle equation is obtained by

$$(x - x_c)^2 + (y - y_c)^2 = r^2 \qquad \text{(A. 6)}$$

where

$$\begin{aligned}
x_c &= \frac{-d_1 + \sqrt{(d_1)^2 - c_1e_1}}{c_1} \\
y_c &= m_5x_c + n_5 \\
r &= k_1(y_c - m_1x_c - n_1) \\
c_1 &= (k_1)^2((m_5)^2 - 2m_1m_5 + (m_1)^2) - (m_5)^2 - 1 \\
d_1 &= (k_1)^2(m_5n_5 - m_5n_1 - m_1n_5 + m_1n_1) \\
&\quad -m_5n_5 + m_5y_3 + x_3 \\
e_1 &= (k_1)^2((n_5)^2 - 2n_1n_5 + (n_1)^2) \\
&\quad -(n_5)^2 + 2n_5y_3 - (x_3)^2 - (y_3)^2
\end{aligned}$$

(iii) The tangential lines l_2 and l_3 are obtained.

The tangential lines l_2 and l_3 go through the points A_0, A_2, respectively and they contact with the circle (A. 6). Then the equations of the straight lines l_2, l_3 are derived by

$$l_2\colon y = m_6x + n_6 \qquad \text{(A. 7)}$$

$$l_3\colon y = m_7x + n_7 \qquad \text{(A. 8)}$$

where

$$\begin{aligned}
m_6 &= \frac{d_2 + \sqrt{(d_2)^2 - c_2e_2}}{c_2} \\
n_6 &= -m_6x_0 + y_0 \\
c_2 &= 2x_cx_0 + r^2 - (x_c)^2 - (x_0)^2 \\
d_2 &= -x_cy_c + x_cy_0 - x_0y_0 + y_cx_0 \\
e_2 &= 2y_cy_0 - (y_0)^2 - (y_c)^2 + r^2
\end{aligned}$$

and

$$\begin{aligned}
m_7 &= \frac{d_3 - \sqrt{(d_3)^2 - c_3e_3}}{c_3} \\
n_7 &= -m_7x_2 + y_2 \\
c_3 &= 2x_cx_2 + r^2 - (x_c)^2 - (x_2)^2 \\
d_3 &= -x_cy_c + x_cy_2 - x_2y_2 + y_cx_2 \\
e_3 &= 2y_cy_2 - (y_2)^2 - (y_c)^2 + r^2
\end{aligned}$$

As mentioned above, the equation of the circular arc connecting the point R, Q at which the arc touches the straignt lines l_1 and l_2, respectively is derived. Then the objective locus of the robot arm is generated.

Appendix B. Derivation of Objective Trajectory at Straight Line Part

The objective trajectory generation is divided into two parts, i.e., the maximum joint acceleration part in the joint coordinates and the maximum speed part within the speed constraint in the working coordinates. The procedure of the objective trajectory generation at straight line is explained as follows.

(i) Maximum joint acceleration part in the joint coordinates

The straight line part is divided into n segments with the constant interval. The segment between the knot point k ($k = 0, 1, 2, \cdots n-1$) and $k+1$ is moved at the maximum joint acceleration. From the equation $\theta_{j,k+1} = \theta_{j,k} + \dot{\theta}_{j,k}h_{j,k} + a_j(h_{j,k})^2/2$, the minimum time $h_{j,k}$ from the joint angle $\theta_{j,k}$ to $\theta_{j,k+1}$ is given by

$$h_{j,k} = \frac{-\dot{\theta}_{j,k} + \sqrt{(\dot{\theta}_{j,k})^2 + 2a_j(\theta_{j,k+1} - \theta_{j,k})}}{a_j}$$

where j ($j = 1, 2$) is the joint number and a_j is

$$a_j = \begin{cases} a_{max} & (\theta_{j,k+1} > \theta_{j,k}) \\ -a_{max} & (\theta_{j,k+1} < \theta_{j,k}) \\ 0 & (\theta_{j,k+1} = \theta_{j,k}) \end{cases}$$

and a_{max}[rad/s^2] is the maximum joint acceleration. The minimum time $h_{j,k}$ is selected at the maximum value of $h_{j,k}$ ($j = 1, 2$) to avoid the torque saturation absolutely. Then the actual time can be expressed by h_k and the trajectory between the knot point k and $k+1$ is generated using the time h_k. The joint acceleration is obtained as

$$\ddot{\theta}_{j,k} = \frac{2(\theta_{j,k+1} - \theta_{j,k} - \dot{\theta}_{j,k}h_k)}{(h_k)^2}$$

and the generated trajectory is derived by

$$\theta_j(t_k + t) = \theta_{j,k} + \dot{\theta}_{j,k}t + \ddot{\theta}_{j,k}t^2/2 \qquad (0 \le t \le t_{k+1} - t_k) \qquad \text{(B. 1)}$$

where $\theta_{j,k}$, $\dot{\theta}_{j,k}$ and $\ddot{\theta}_{j,k}$ are the joint angle, joint velocity and joint acceleration, respectively for each jth axis and kth step, and t_k is the time at the knot point k.

(ii) Maximum speed part within the speed constraint in the working coordinates

The trajectory from the starting point to the end point is generated by (B. 1), and the velocity and the time at one sampling before the tangential speed exceeds the speed constraint v_{max} are denoted by v_ρ and t_ρ. Similarly, the trajectory from the end point to the starting point is generated, and the the velocity and the time at one sampling before the tangential speed exceeds the speed constraint v_{max} are assumed to be v_σ and t_σ. The interval l_c of the maximum speed part is derived by

$$l_c = \sqrt{(x(t_\sigma) - x(t_\rho))^2 + (y(t_\sigma) - y(t_\rho))^2}$$

The transit time t_c and the acceleration A_c at the maximum speed part can be derived easily as $t_c = 2l_c/(v_\rho + v_\sigma)$ and $A_c = (v_\sigma - v_\rho)/t_c$. The trajectory at the maximum speed part is generated.by

$$x(t) = x(t_\rho) + \dot{x}(t_\rho)(t - t_\rho) + A_c \cos\phi (t - t_\rho)^2/2 \quad (t_\rho \le t \le t_\sigma) \qquad \text{(B. 2)}$$

$$y(t) = y(t_\rho) + \dot{y}(t_\rho)(t - t_\rho) + A_c \sin\phi (t - t_\rho)^2/2 \quad (t_\rho \le t \le t_\sigma) \qquad \text{(B. 3)}$$

where $\phi = \sin^{-1}((y(t_\sigma) - y(t_\rho))/l_c)$. The trajectory (B. 2), (B. 3) in the working trajectory is transformed into the trajectory in the joint coordinates by the inverse kinematics, and the joint trajectory is obtained.

According to the above procedure, the objective trajectory at the straight line part is generated.

Masatoshi Nakamura (Member)

Masatoshi Nakamura was born in 1943. He received B.S., M.S. and Ph.D. degrees in Electrical Engineering from Kyushu University, in 1967, 1969 and 1974, respectively. From 1973 to 1974, he was a Research Associate in Kyushu University. Since 1974, he has been with the Faculty of Science and Engineering, Saga University, where he was a lecturer from 1974 to 1975, an Associate Professor from 1975 to 1987, a Professor from 1988 to 1997, in Department of Electrical Engineering, and a Professor since 1988, in the Department of Advanced Systems Control Engineering. His research interests include systems control theory and its applications, especially power system control, thermal flow-control, robotics and biomedical engineering. Prof. Nakamura is a fellow of the Society of Instrument and Control Engineers of Japan, and a member of the IEEE Control Systems Society, the Institute of Electrical Engineers of Japan.

Takuya Iwanaga (Student Member)

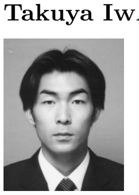

Takuya Iwanaga was born in 1978. He received B.S. degree in Electrical Engineering from Saga University in 2000. Currently, he is pursuing M.Sc. degree in the department of Advanced Systems Control Engineering. His research interest focuses on mechatronic systems control.

Satoru Goto (Member)

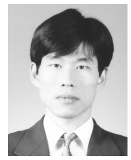

Satoru Goto was born in 1966. He received B.S. and M.S. degrees in applied physics from Osaka University, Osaka, Japan, in 1988 and 1990, respectively, and Ph.D degree from Osaka University in 1995. Since 1995, he has been with the Faculty of Science and Engineering, Saga University, Saga, Japan, where he was a Research Associate from 1995 to 1996, a lecturer from 1996 to 1998 and an Associate Professor since 1998, in the Department of Advanced Systems Control Engineering. His research interests include control theory and its applications to actual systems. Dr. Goto is a member of of IEEE, the Robotics Society of Japan, the Institute of Systems, Control and Information of Japan.

Nobuhiro Kyura (Member)

Nobuhiro Kyura was born in 1942. He received B.S., M.S. and Ph.D. degrees in electrical engineering from Kyushu University in 1964, 1966 and 1992, respectively. Since 1964, he has been with Yaskawa Electric Corporation, Japan, where he is currently the consultant of the Research Laboratory. Since 1995, he has been with the Department of Electrical Engineering, Kinki University (Kyushu), where he is currently a Professor in the Department of Electrical Engineering. His research interests include motion controller architecture, optimum motion control and robot manipulator control. He is a member of the Institute of Electrical Engineers of Japan, the Society of Instrument and Control Engineers of Japan and the Institute of Systems, Control and Information of Japan.

Reprinted from Trans. of the SICE
Vol. 37 No. 4 338/345 2001